

Article

Resin- and magnetic nanoparticle-based free radical probes for glycan capture, isolation, and structural characterization

Kimberly Fabijanczuk, Kaylee Gaspar, Nikunj Desai, Jungeun Lee, Daniel A. Thomas, Jesse Lee Beauchamp, and Jinshan Gao

Anal. Chem., **Just Accepted Manuscript** • DOI: 10.1021/acs.analchem.9b01303 • Publication Date (Web): 13 Nov 2019

Downloaded from pubs.acs.org on November 18, 2019

Just Accepted

"Just Accepted" manuscripts have been peer-reviewed and accepted for publication. They are posted online prior to technical editing, formatting for publication and author proofing. The American Chemical Society provides "Just Accepted" as a service to the research community to expedite the dissemination of scientific material as soon as possible after acceptance. "Just Accepted" manuscripts appear in full in PDF format accompanied by an HTML abstract. "Just Accepted" manuscripts have been fully peer reviewed, but should not be considered the official version of record. They are citable by the Digital Object Identifier (DOI®). "Just Accepted" is an optional service offered to authors. Therefore, the "Just Accepted" Web site may not include all articles that will be published in the journal. After a manuscript is technically edited and formatted, it will be removed from the "Just Accepted" Web site and published as an ASAP article. Note that technical editing may introduce minor changes to the manuscript text and/or graphics which could affect content, and all legal disclaimers and ethical guidelines that apply to the journal pertain. ACS cannot be held responsible for errors or consequences arising from the use of information contained in these "Just Accepted" manuscripts.

Resin- and magnetic nanoparticle-based free radical probes for glycan capture, isolation, and structural characterization

Kimberly Fabijanczuk,^a Kaylee Gaspar,^a Nikunj Desai,^a Jungeun Lee,^a Daniel A. Thomas,^b J. L. Beauchamp,^{b*} Jinshan Gao^{a*}

^a Department of Chemistry and Biochemistry, and Center for Quantitative Obesity Research, Montclair State University, Montclair, NJ 07043, gaoj@montclair.edu

^b Arthur Amos Noyes Laboratory of Chemical Physics, California Institute of Technology, Pasadena, CA 91125, jlbchamp@caltech.edu

ABSTRACT: By combining the merits of solid supports and free radical activated glycan sequencing (FRAGS) reagents, we develop a multi-functional solid-supported free radical probe (SS-FRAGS), which enables glycan enrichment and characterization. SS-FRAGS comprises a solid support, free radical precursor, disulfide bond, pyridyl, and hydrazine moieties. Thio-activated resin and magnetic nanoparticles (MNPs) are chosen as the solid support to selectively capture free glycans via the hydrazine moiety, allowing for their enrichment and isolation. The disulfide bond acts as a temporary covalent linkage between the solid support and the captured glycan, allowing the release of glycans via the cleavage of the disulfide bond by dithiothreitol. The basic pyridyl functional group provides a site for the formation of a fixed charge, enabling detection by mass spectrometry and avoiding glycan rearrangement during collisional activation. The free radical precursor generates a nascent free radical upon collisional activation and thus simultaneously induces systematic and predictable fragmentation for glycan structure elucidation. A radical-driven glycan deconstruction diagram (R-DECON) is developed to visually summarize the MS² results and thus allow for the assembly of the glycan skeleton, making the differentiation of isobaric glycan isomers unambiguous. For application to a real-world sample, we demonstrate the efficacy of the SS-FRAGS by analyzing glycan structures enzymatically cleaved from RNase-B.

INTRODUCTION

Glycosylation is one of the most important forms of protein post-translational modification, and it plays a vital role in biology. The analysis of glycans by mass spectrometry has been hampered by the trace amounts of glycan sample available from low-abundant glycoconjugates in biological sources. Alterations of glycan structures have been found in various types of diseases, such as cancers, diabetes, and immune disorders.¹⁻² Therefore, profiling disease-associated glycans is essential for the understanding of their functions at a molecular level, while also facilitating the identification of diagnostic glycan biomarkers and the better design of therapeutic drugs. Mass spectrometry (MS) has proven to be the most powerful and informative tool to elucidate glycan structures and inform their roles in biological processes. Prior to mass spectrometric analysis, glycan samples are prepared mainly in three steps: 1) glycoprotein isolation and/or digestion; 2) glycan release from glycoproteins; 3) glycan enrichment from the mixture, which consists of proteins, peptides, enzymes, and other chemicals involved in sample preparation. It is challenging to directly analyze glycans with even traces of these other components by MS since some species, such as proteins and peptides, are often much more readily ionized, and thus greatly suppress glycan ionization and detection. As a result, efficient glycan enrichment and separation from complex biological mixtures is crucial for mass spectrometric glycan characterization. Physical interaction based approaches, including lectin affinity chromatography,³⁻⁶ hydrophilic interaction liquid chromatography (HILIC),⁷⁻¹⁴ and graphite affinity chromatography^{7, 10, 15-16} have been widely utilized to enrich glycans from complex biological samples. Unfortunately, nonspecific binding and low enrichment efficiency often mitigate their effective application. Solid-phase chemical immobilization methods have emerged as promising alternatives for glycan enrichment.¹⁷⁻²⁵ After either enzymatic release or chemical release by β -elimination from glycoproteins, glycans have a single reducing terminus, which has both cyclic and open forms. The reducing terminus can covalently conjugate with hydrazide, amine, and oxyamine functionalities through its unique aldehyde functional group in its open form.^{17, 19, 26}

Mass spectrometric glycan structure elucidation is extremely challenging. Glycans can exhibit incredibly complicated branched structures with a large number of residues having both structural and stereochemical diversity. It has been stated that “small changes in environmental cues can cause dramatic changes in glycans produced by a given cell”.²⁷ Although significant advances have been made, glycomics remains much less developed than its siblings, genomics and

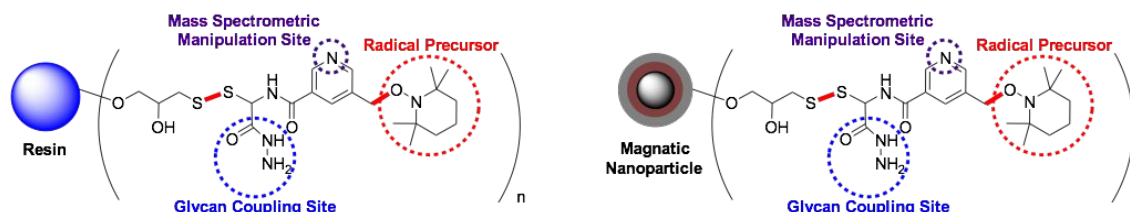
1
2
3 proteomics. Noted for its capability to perform multi-stage tandem mass spectrometry, minimal
4 sample consumption, and high sensitivity, mass spectrometry has been broadly used for the
5 elucidation of glycan structures. Many dissociation techniques, such as collision-induced
6 dissociation (CID),²⁸⁻³⁰ infrared multiphoton dissociation (IRMPD),^{29, 31} higher-energy collisional
7 dissociation (HCD),^{23, 32} ultraviolet multiphoton dissociation,³³⁻³⁵ electron capture dissociation
8 (ECD),^{29, 36-38} electron transfer dissociation (ETD),³⁹⁻⁴⁰ electron detachment dissociation (EDD),<sup>29,
9 39, 41-43</sup> and electron excitation dissociation (EED),⁴³⁻⁴⁵ have been demonstrated to provide
10 complementary and extensive information for glycan structural analysis. Among these dissociation
11 techniques, ECD, ETD, EDD, and EED are generally referred to as electron activated dissociation
12 (ExD) since they usually involve fragmentation via low energy free radical dissociation pathways.
13 ExD provides enhanced yields of cross ring fragmentations. However, such approaches require
14 special instrumentation to allow for interaction of an electron source with targeted ions. Recently,
15 free radical chemistry⁴⁶ has regained great attention in the field of biomolecular characterization.<sup>47-
16 51</sup>

17
18
19 Inspired by the achievement of electron activated dissociation (ExD) for glycan structure analysis,
20 which usually involve fragmentation via low energy free radical dissociation pathways, we
21 recently developed a novel free radical activation glycan sequencing reagent (FRAGS), along with
22 a methylated free radical activated glycan sequencing reagent (Me-FRAGS) for glycan structural
23 characterization.^{26, 52} Free radical-directed systematic glycan dissociation with high fragmentation
24 efficiency has been obtained using these two free radical reagents. Moreover, the use of these free
25 radical glycan sequencing reagents does not require multiply charged precursor ions. Furthermore,
26 our reagents can be employed with a wide variety of instrumentation, with the main requirement
27 being the availability of collisional activation of mass selected ions to achieve fragmentation.
28 However, use of these two reagents is hampered by the low sensitivity for glycan detection when
29 applied to glycans released enzymatically from glycoproteins, subsequently coupled with the
30 FRAGS or Me-FRAGS reagent, and then directly analyzed by mass spectrometry without any
31 enrichment or purification. Proteins and peptides, which are the major matrix, significantly
32 suppress the ionization of glycans.

33
34 For solid supports, we employ thio-activated resin beads and magnetic nanoparticles (MNPs).
35 Resin beads and magnetic nanoparticles (MNPs) have been broadly used as solid-supports and
36
37
38
39
40
41
42
43
44
45
46
47
48
49
50
51
52

1
2
3 receive significant attention for their potential biomedical applications, such as sample purification
4 and enrichment.^{25, 53-57} Thiol-activated resin (Thiopropyl Sepharose™ 6B) is a medium for
5 reversible immobilization of molecules containing thiol groups under mild conditions via the
6 formation of a disulfide bond. For instance, it has been commonly used to enrich thiol-containing
7 compounds including thiolated proteins, thiolated peptides, thiolated RNA, thiophosphates, and
8 aliphatic thiols. More recently, attempts have been made to exploit its reactivity with thiols to
9 generate resin-supported probes for the analysis of biomolecules.²⁵ However, the relatively low
10 surface-to-volume ratio and large particle size (100 μm) of resin hinders its further application in
11 the biomedical field, especially for in vivo diagnosis and therapy. Magnetic nanoparticles (MNPs)
12 have attracted much attention due to their high magnetic susceptibility, biocompatibility, and
13 stability, along with other important relevant characteristics. Their unique physical properties
14 make MNPs the ideal medium for in vivo biomedical applications, such as drug delivery,
15 hyperthermia treatment, and magnetic resonance imaging (MRI) of cancer cells.⁵⁸ Considering the
16 potential biomedical application of SS-FRAGS, we designed and prepared both resin- and MNPs-
17 supported free radical probes.
18

19 Overall, glycan structural intricacy, low abundance, and masked detection are the main barriers to
20 direct application of our sequencing reagents to real world analyses. To address these issues, we
21 have developed a multi-functional solid-supported free radical probe (SS-FRAGS, Scheme 1). The
22 probe comprises of a solid support, disulfide bond, free radical precursor, pyridyl, and hydrazine
23 moieties. SS-FRAGS selectively captures free glycans, allowing for their enrichment and
24 purification. The disulfide bond acts as a temporary covalent linkage between the solid support
25 and the free radical reagent, allowing the release of glycans via the cleavage of this bond after
26 enrichment and purification. The free radical precursor generates a nascent free radical upon
27 collisional activation, which subsequently initiates low energy free radical dissociation pathways,
28 fragmenting the glycan. The pyridyl functional group provides a fixed charge, allowing glycan
29 structure determination from analysis of the systematic fragmentation of the glycan back towards
30 the reducing terminus. The hydrazine functional group selectively targets bioconjugation with the
31 reducing terminus of the glycan, serving as a coupling site between the reagent and the glycan.
32
33
34
35
36
37
38
39
40
41
42
43
44
45
46
47
48
49
50
51
52
53
54
55
56
57
58
59
60



Scheme 1. Structures of solid-supported free radical probes.

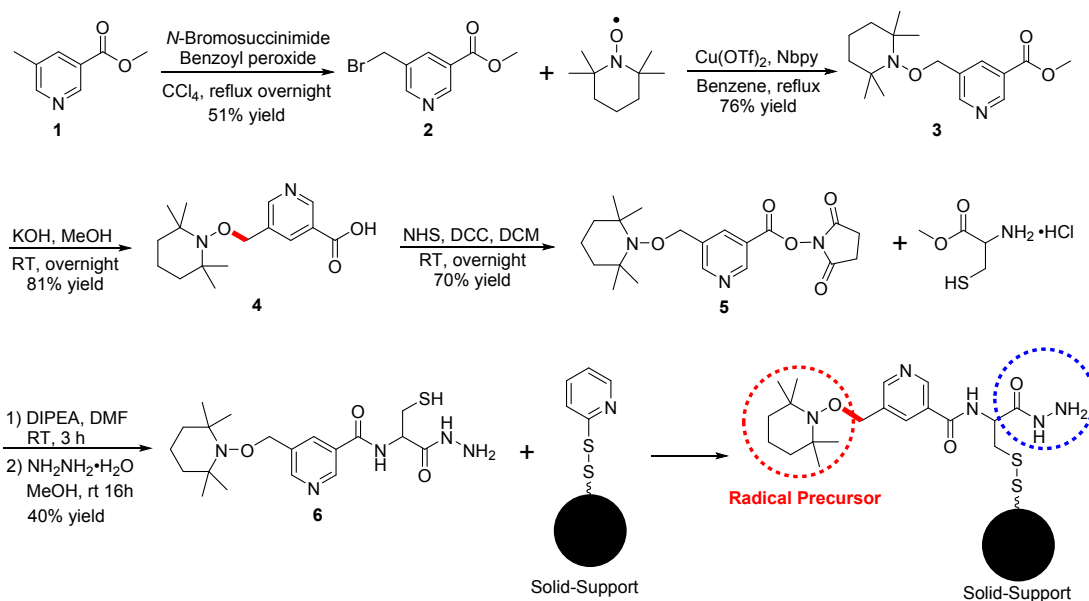
EXPERIMENTAL SECTION

Glycans

Lacto-*N*-difucohexaose I (LNDFH I), lacto-*N*-difucohexaose II (LNDFH II), and Ribonuclease B (RNase B) from bovine pancreas were purchased from Sigma-Aldrich (St. Louis, MO, USA). Iron(III) chloride hexahydrate and iron(II) chloride tetrahydrate were purchased from Alfa Aesar (Tewksbury, MA, USA). All solvents are HPLC grade and were purchased from EMD Merck (Gibbstown, NJ, USA). All other chemicals were purchased from Sigma-Aldrich (St. Louis, MO, USA).

Preparation of Solid-Supported Free Radical Probes

The preparation of the solid-supported free radical probe (SS-FRAGS) is described with details in the supporting information (Scheme 2). Briefly, the synthesis of SS-FRAGS is accomplished by benzylic bromination with NBS, coupling with NBS, hydrolysis of the ester group, condensation between the carboxylic acid and cysteine, hydrazinolysis of the imide group, and finally disulfide bond formation between the resin coupling reagent and thiol activated resin.^{26, 52} The preparation of magnetic nanoparticle (Scheme S1) was achieved by following previously reported procedures.⁵⁹ Electron microscopy reveals the average size of the magnetic nanoparticles as 10 nm (Figure S1).



Scheme 2. Preparation of the solid-supported free radical probe (SS-FRAGS).

Mass Spectrometry

A Thermo-Fisher Scientific linear quadrupole ion trap (LTQ-XL) mass spectrometer (Thermo, San Jose, CA, USA) equipped with an electrospray ionization (ESI) source was employed. Derivatized glycan sample solutions were directly infused into the ESI source of the mass spectrometer via a syringe pump at a flow rate of 5–10 $\mu\text{L}/\text{min}$. Critical parameters of the mass spectrometer include spray voltage of 5–6 kV, capillary voltage of 30–40 V, capillary temperature of 275 $^{\circ}\text{C}$, sheath gas (N_2) flow rate of 10 (arbitrary unit), and tube lens voltage of 80–200 V. Other ion optic parameters were optimized by the auto-tune function in the LTQ-XL tune program for maximizing the signal intensity. Collision-induced dissociation (CID) was performed by resonance excitation of the selected ions for 30 milliseconds. The normalized CID energy was 10–45 (arbitrary unit).

RESULTS AND DISCUSSION

All product ions are classified according to the Domon and Costello nomenclature.⁶⁰ Greek letters α and β are employed to differentiate a branched glycan wherein α indicates the heavier branch while β indicates the lighter branch.

Glycan Characterization

To test the capability of both resin- and MNPs-supported free radical probes for glycan structure elucidation, maltopentaose and one pair of isobaric glycan isomers, lacto-*N*-difucohexaose I (LNDFH I) and lacto-*N*-difucohexaose II (LNDFH II), were selected. Maltopentaose presents a

linear chain of five identical glucose residues. LNDFH I and II are branched difucosylated hexasaccharides differing only in the location of the terminal fucose residue.

Maltopentaose: The general procedure for glycan purification and enrichment is illustrated in Figure 1. Briefly, glycans are selectively captured through covalent conjugation to the SS-FRAGS via the reduction reaction between the unique glycan reducing terminus and the probe hydrazide moiety (glycan coupling site of the probe, Figure 1). To achieve glycan purification and enrichment, the impurities and/or excess reactants are thoroughly washed away by water and acetonitrile. After enrichment, the conjugated glycans are released by the selective cleavage of the disulfide bond using the chemical scissors, dithiothreitol (DTT). Then, the conjugated glycans are methylated by reacting with iodomethane at the pyridine nitrogen site to avoid glycan rearrangement during collisional activation, ionized by electrospray ionization (ESI), and subjected to collision-induced dissociation (CID) in the ion trap.

As expected, collisional activation generates systematic and predictable glycan dissociation (Z, Y, and $^{1,5}X$) with the charge retained on the reducing terminus, which significantly decreases the complexity of the CID spectra (Figure 2). The nascent free radical is generated by the loss of TEMPO at the radical precursor site. Without the need for subsequent collisional activation, all ions resulting from glycan fragmentation are generated via a free radical initiated mechanism. The formation of these three types of ions are proposed to result from hydrogen abstraction, initiated by the nascent free radical, followed by a series of β -eliminations.^{26, 52} The free radical activated glycan dissociation is systematic and predictable due to the narrow range of the C–H bond dissociation enthalpies (BDEs) of the glycan.^{26, 52}

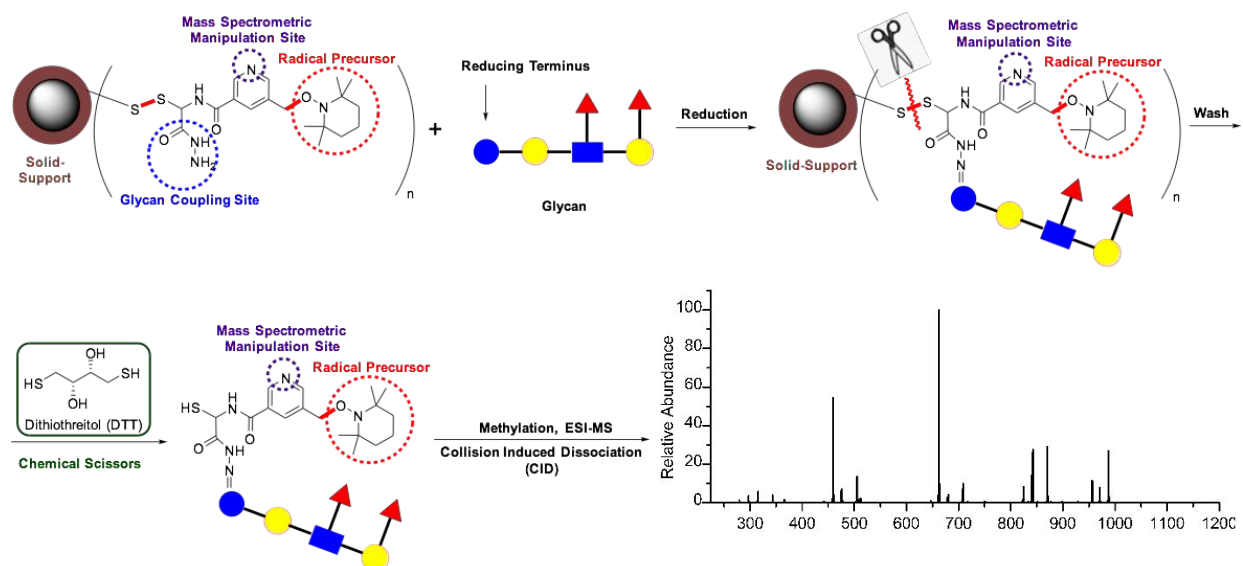


Figure 1. Schematic diagram of glycan capture, release, and MS analysis.

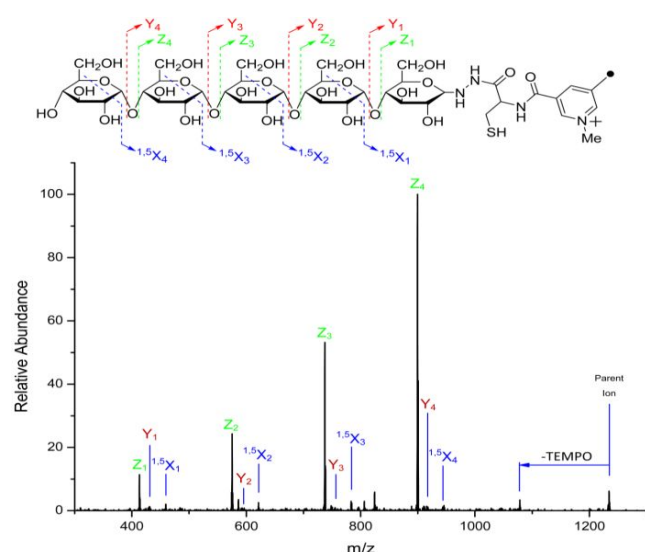


Figure 2. The fragmentation patterns and MS² CID spectrum of SS-FRAGS-derivatized maltopentaose.

LNDFH I and II: LNDFH I and II were employed as highly branched isobaric glycans to assess the capability of SS-FRAGS to analyze more complicated glycan structures and differentiate glycan isomers. Similarly, systematic and predictable radical-directed glycan fragment ions are generated upon collisional activation, including Z, Y, ^{1,5}X, and Z_α+Z_β ions retaining the charge on the reducing terminus. More importantly, the unique fragmentation pattern Z_α+Z_β (Z_{3α}+Z_{3β} for LNDFH I and Z_{1α}+Z_{1β} and Z_{3αα}+Z_{3αβ} for LNDFH II, Figure 3) is observed only at the branch site, providing the information to confirm the presence and location of the branch structure. It is

essential to note that the two glycosidic linkages need to be adjacent to each other to observe the unique $Z_{\alpha}+Z_{\beta}$ ion. The glycan LNDFH I has β 1-3 and α 1-4 linkages on the branch site while LNDFH II has α 1-3 and β 1-4 linkages on the first branch site and β 1-3 and α 1-4 linkages on the second branch site. The determination of branch sites with two glycosidic linkages which are not adjacent to each other will be discussed in the case of glycans released from RNase B (*vide infra*). The mechanism for the formation of this unique ion has been proposed to be hydrogen abstraction followed by β -elimination.²⁶ Meanwhile, the radical-driven glycan deconstruction diagram (R-DECON diagram, Figure 4) visually summarizes the MS² results and thus allows for the assembly of the glycan skeleton, making the differentiation of these two isobaric glycan isomers unambiguous.

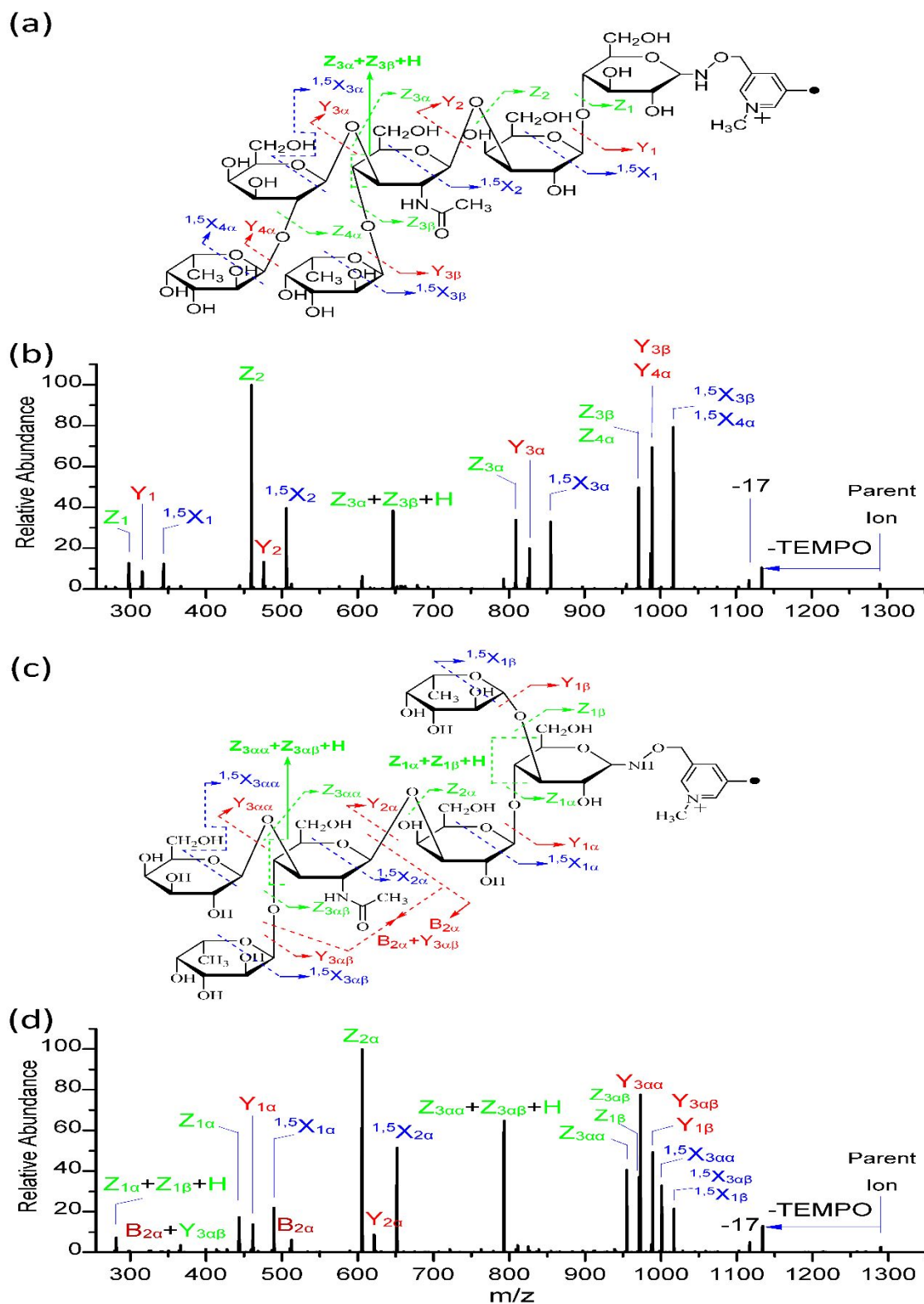


Figure 3. The fragmentation patterns observed following MS² CID of MNPs-FRAGS-derivatized LNDFH I (a), LNDFH II (c), and the CID spectra of MNPs-FRP-derivatized LNDFH I (b), LNDFH II (d).

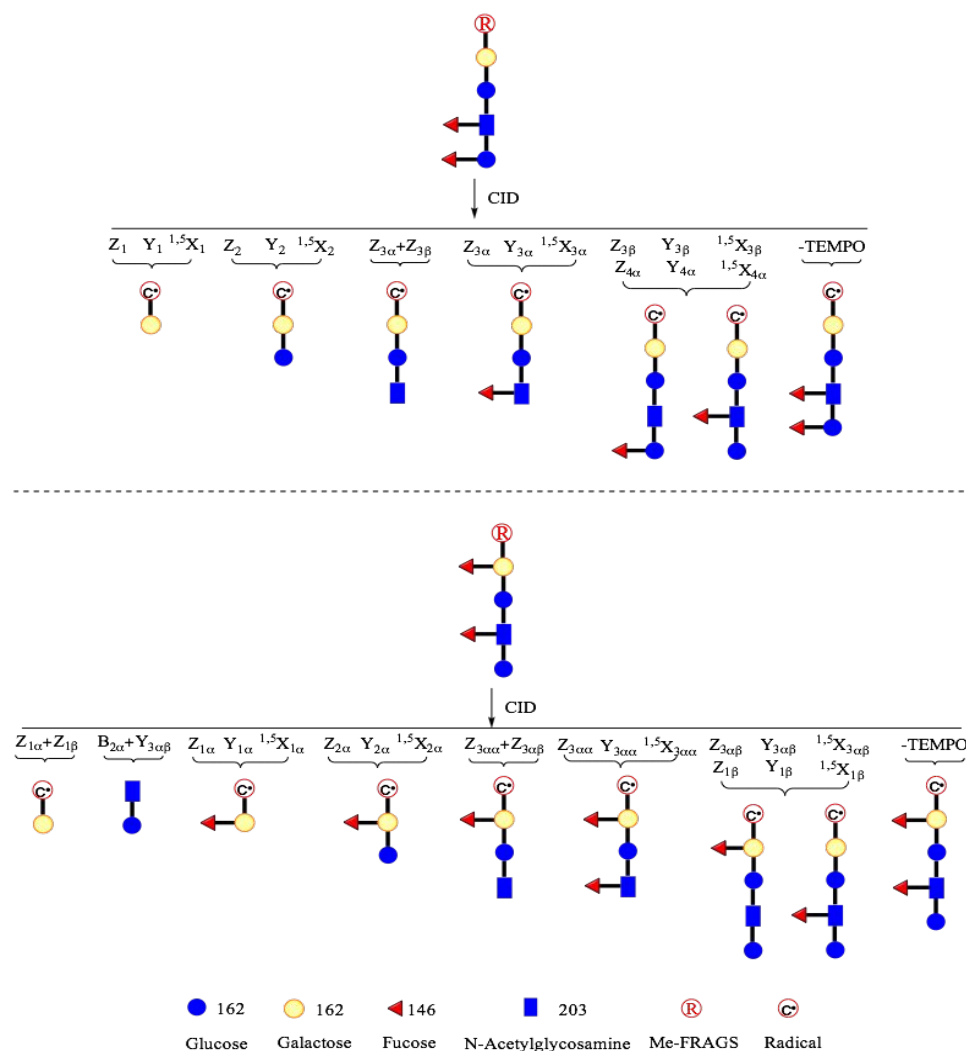


Figure 4. Radical-driven glycan deconstruction (R-DECON) diagrams for LNDFH I and II. In each case the precursor ion is subjected to MS² to generate a series of product ions, allowing the assembly of the glycan skeleton and differentiation of these two isobaric glycan isomers.

Glycan Enrichment

To test the capability of SS-FRAGS for the enrichment of glycans from biological samples, analysis of glycans released from Ribonuclease B (RNase B) from bovine pancreas was performed. Bovine pancreatic RNase B is a glycoprotein that contains a single glycosylation site at Asn³⁴. Due to the heterogeneity in the glycosylation at Asn³⁴, RNase B has five glycosylated variants, with an average molecular weight of approximately 15 kDa. The general procedure for glycan purification and enrichment is illustrated in Figure S2. The RNase B (1 mg) was denatured at 90 °C for one hour. Then the glycans were enzymatically released from RNase B by PNGase F followed by the enrichment protocol described in Figure 1. Briefly, without any pre-purification, the SS-FRAGS

1
2
3 reagent selectively captures the glycans to the probe via the reductive coupling reaction. Glycan
4 enrichment is achieved by simply washing all the impurities away with water and acetonitrile. The
5 pyridyl functional group of the probe is then reacted with iodomethane to form a fixed positive
6 charge. Finally, the disulfide bond is cleaved by dithiothreitol (DTT) to release the derivatized
7 glycans for mass spectrometric analysis.
8
9

10
11
12 By utilizing SS-FRAGS and following the procedure described in the protocol above, all the
13 impurities including proteins, peptides, salt, and detergent were easily washed away by water and
14 acetonitrile, allowing the purification and enrichment of glycans. As shown in Figure 5, abundant
15 ions were detected, enabling subsequent collision induced dissociation for further structure
16 characterization of glycans released from RNase B, which is further discussed below. FRAGS (b,
17 Figure 5), which were proved to provide systematic and predictable cleavages for glycan structure
18 elucidation, were used as a point of comparison to prove the capability of solid-supported free
19 radical probe to enrich glycans. No signal was observed for the parallel control test (b, Figure 5).
20 To further compare SS-FRAGS with SPE, we run the SPE purification after derivatization of
21 FRAGS. It is clear that SS-FRAGS obtains better glycan purification than SPE.
22
23
24
25
26
27
28
29
30
31
32
33
34
35
36
37
38
39
40
41
42
43
44
45
46
47
48
49
50
51
52
53
54
55
56
57
58
59
60

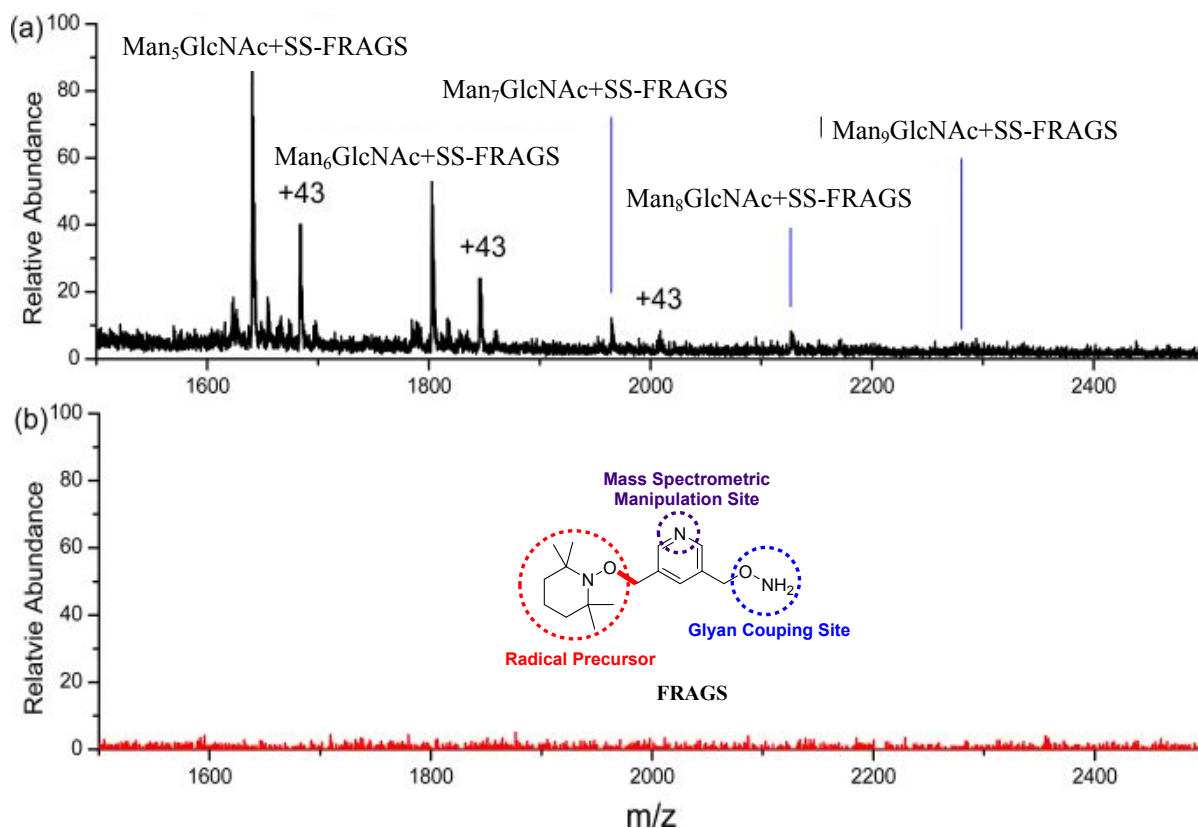


Figure 5. Enrichment of glycans released from RNase B by SS-FRAGS (a), and control test by using FRAGS (b).

Abundant mass spectrometric signals were observed for target glycans which were released from RNase B. It has been reported that the high-mannose structures released from RNase B exist as a mixture of isomers.^{61, 62} For instance, three permethylated Man₇GlcNAc₂ isomers have been reported by using porous graphite LC/MS (quadrupole orthogonal time-of-flight mass spectrometer).⁶¹ Moreover, ion trap mass spectrometry has been reported to define RNase B glycan topology and isomers by coupling precursor isolation with sequential MSⁿ disassembly.⁶² Generally, prior separation of the glycans before structural analysis is certainly desirable, since isobaric isomers can often be resolved and characterized individually. We tried to use HPLC to separate derivatized glycans and found that the two isomers from the coupling of the reagent to the reducing end of the glycan, adding complexity to the use of HPLC by increasing the number of peaks. This can be rationalized by considering the α and β forms of the reducing terminus. Reduction after amination was also tried to avoid the α and β forms but cannot be achieved. Without the prior HPLC separation, further collisional activation was still conducted to induce fragmentation for structural elucidation of the most abundant isomers of glycans released from

1
2
3 RNase B, as illustrated below. The free radical probes developed here provide more structural
4 information to further elucidate the structures of the most abundant isomer of glycans released
5 from RNase B. Figure 6 shows the CID mass spectra of free radical probe derivatized glycans
6 released from RNase B. As expected, only systematic Z, Y, and 1,5 X cleavages were generated due
7 to the presence of the well-defined site of radical generation. The R-DECON diagram makes
8 possible the straightforward visualization of the assembly of the glycan skeleton (Figure 7). For
9 instance, the proposed structure of the most abundant isomer of $\text{Man}_5\text{GlcNAc}_2$ can be confirmed
10 by the loss of one mannose, three mannose, and five mannose residues, as shown in Figure 6. We
11 have reported the unique ion, $Z_\alpha + Z_\beta$, for the adjacent branch site of glycans, such LNDHF I and
12 II.^{26, 52} The disappearance of the $Z_\alpha + Z_\beta$ ions indicates the two glycosidic linkages in the branch
13 site are distal to each other. However, the branch sites can still be determined by analyzing the
14 fragmentation patterns since each fragment ion is a product of single cleavages (Z, Y, and 1,5 X)
15 induced by the nascent free radical. The loss of five mannose residues indicates the cleavage of
16 the glycosidic bond between the mannose and *N*-acetylglucosamine (GlcNAc). The losses of one
17 and three mannose subunits denote that one mannose residue is on one side and three mannose
18 residues are on the other side of the first branch site. Moreover, the first branch site can also be
19 confirmed by the absence of the loss of four mannose residues. The loss of four mannose residues
20 would indicate the presence of four connected mannose residues which can be released by a single
21 glycosidic bond cleavage, such as the four mannose residues enclosed in the red box in the
22 proposed structure of $\text{Man}_5\text{GlcNAc}_2$ (**a** and **b** in Figure 8). Meanwhile, the second branch site is
23 determined by the absence of the loss of two mannose residues. The loss of two mannose residues
24 would indicate the presence of two mannose residues which can be released by a single glycosidic
25 bond cleavage, such as the two mannose residues enclosed in the blue box in the proposed structure
26 of $\text{Man}_5\text{GlcNAc}_2$ (**a**, **b**, and **c** in Figure 8). As expected, MS² CID generates one mannose, two
27 mannose, three mannose, and six mannose losses for the most abundant isomers of $\text{Man}_6\text{GlcNAc}_2$.
28 The presence of two and three mannose residue losses provides information to decipher the
29 composition of the first branch site: two mannose residues on one side and three on the other side.
30 Again, the first branch site configuration can be confirmed by the absence of the loss of four or
31 five mannose residues. Two structures have been proposed for $\text{Man}_6\text{GlcNAc}_2$. Unfortunately, the
32 existence of the second branch site cannot be confirmed due to the fact that these two proposed
33 glycans can have the same radical directed fragmentation patterns. Similarly, two structures have
34
35
36
37
38
39
40
41
42
43
44
45
46
47
48
49
50
51
52
53
54
55
56
57
58
59
60

been proposed for the most abundant isomers of $\text{Man}_7\text{GlcNAc}_2$. Three $\text{Man}_7\text{GlcNAc}_2$ isomers have been reported by Costello et. al. by coupling HPLC separation with Q-TOF mass spectrometry.⁶¹ Neither of the Man_7 structures shown in Figure 6c conforms to known biosynthetic knowledge and both structures are likely incorrect. At the present stage, R-DECON can generate the correct structure only for glycan compositions with a single (dominant) isomer. When multiple isomers are present in comparable abundances, R-DECON analysis of the resultant tandem mass spectra containing fragments from all isomers will likely produce the wrong structures, as was the case for $\text{Man}_7\text{GlcNAc}_2$. This limitation may be overcome by performing chromatographic separation prior to MS/MS analysis. The masses of the radical probe derivatized glycans $\text{Man}_8\text{GlcNAc}_2$ and $\text{Man}_9\text{GlcNAc}_2$ exceeded the nominal mass range of the instrument. They were detected but low signal intensity did not provide useful MS² results for these products.

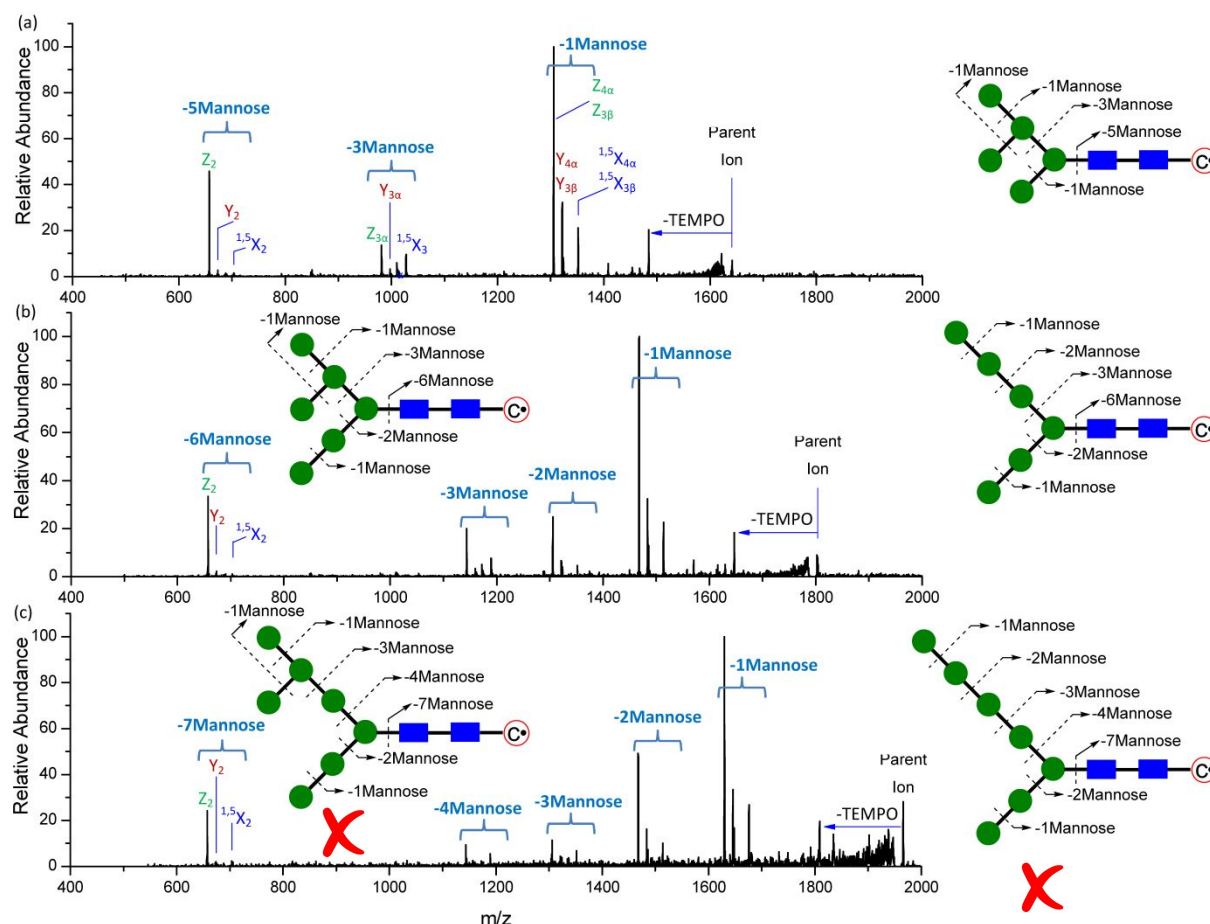


Figure 6. The fragmentation patterns observed following CID of MNPs-FRP-derivatized $\text{Man}_5\text{GlcNAc}_2$ (a), $\text{Man}_6\text{GlcNAc}_2$ (b), and $\text{Man}_7\text{GlcNAc}_2$ (c). Parent ion refers to the methylated molecular ion.

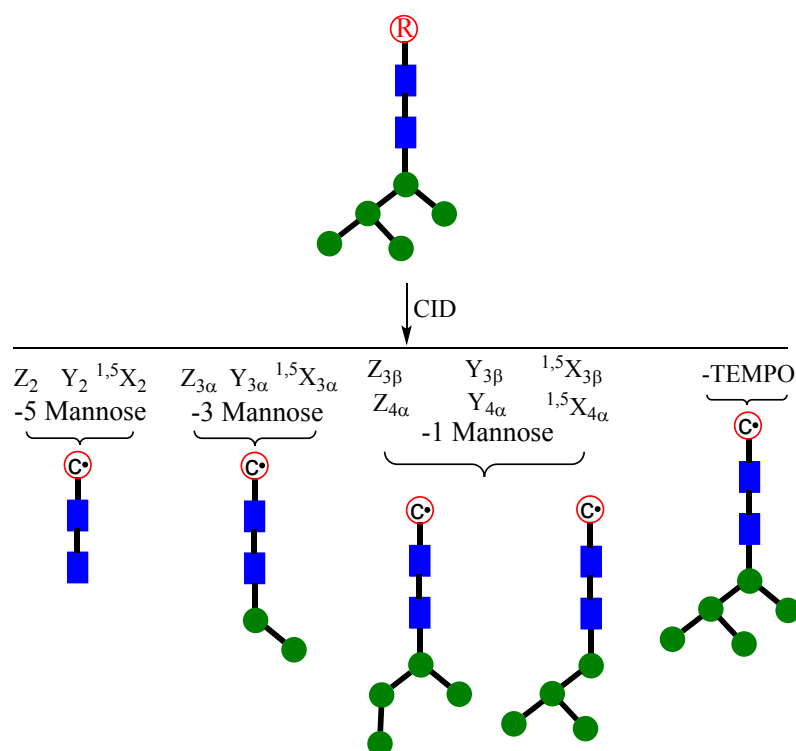


Figure 7. Radical-driven glycan deconstruction (R-DECON) diagram for $\text{Man}_5\text{GlcNAc}_2$.

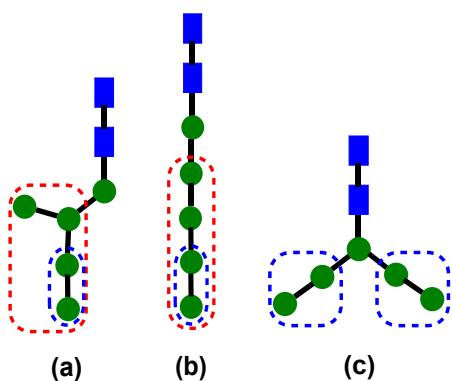


Figure 8. Proposed structures of $\text{Man}_5\text{GlcNAc}_2$ that would be able to lose two (enclosed in blue box) or four (enclosed in red box) mannose residues. Structures (a), containing one branch with one and three mannose residues on two sides, can have loss of two and four mannose residues. Structure (b) with no branches can have loss of two and four mannose residues. Structure (c), containing one branch with two mannose residues on each side, can have loss of two mannose residues.

CONCLUSION

In this study, we describe and demonstrate the effective application of multi-functional solid-supported free radical probes for glycan enrichment and characterization. Glycans which are enzymatically cleaved from proteins can be easily enriched by temporary and selective immobilization on resin beads or magnetic nanoparticles via the reduction reaction between a hydrazide moiety of the probe and the reducing terminus of the target glycans. Glycan characterization is achieved by the systematic and predictable fragmentation induced by a well-defined nascent free radical which is generated following cleavage of the captured glycan from the solid support. Major fragmentation processes include the formation of $^{1,5}X$, Y, and Z ions for both model glycans and glycans released from RNase B. In addition, the unique $Z_{\alpha}+Z_{\beta}$ ions ($Z_{3\alpha}+Z_{3\beta}$ for LNDFH I and $Z_{1\alpha}+Z_{1\beta}$ and $Z_{3\alpha\alpha}+Z_{3\alpha\beta}$ for LNDFH II) can be used for the identification of the branch sites with adjacent linkages, such as the 1-3 and 1-4 linkages on the branch site for LNDFH I. Glycan structures can be visually assembled by the systematic development of radical directed DECON diagrams using MS^n data. The systematic radical-directed fragmentation aids in the determination of glycan structures and in particular facilitates discrimination of isomeric glycans that differ only in the connectivity of their component sugars. The determination of branch sites with two glycosidic linkages which are distal to each other can also be confirmed. For the glycans released from RNase B, the structure of the most abundant isomer of $Man_5GlcNAc_2$ is proposed and validated to have two branch sites with distal glycosidic linkages. The configuration of these two branch sites is confirmed by the corresponding loss of mannose subunits on each side of the branch site. For the most abundant isomers of $Man_6GlcNAc_2$ the configuration of the first branch can be determined, although the existence and/or configuration of the second branch site cannot be ascertained. Chromatographic separation of $Man_7GlcNAc_2$ prior to MS/MS analysis is especially needed since there are three major isomers for $Man_7GlcNAc_2$. The development of new free radical reagent, which allows the HPLC separation without increasing the peak numbers, is underway.

The enhancement of glycan enrichment, high fragmentation efficiency, and systematic radical-directed dissociation facilitates the application of SS-FRAGS in addressing problems in structural glycobiology.

Supporting Information Available: [Details about the preparation of the solid-supported free radical probe (SS-FRAGS), schematic illustration of glycan enrichment and MS analysis using solid-supported free radical probes, and NMR spectroscopy of synthesized compounds]

ACKNOWLEDGEMENTS

This work is supported by the National Institutes of Health through grant 1R15GM121986-01A1, National Science Foundation through grant CHEM1709272, Beckman Institute at Caltech, and National Science Foundation through grant CHEM1508825.

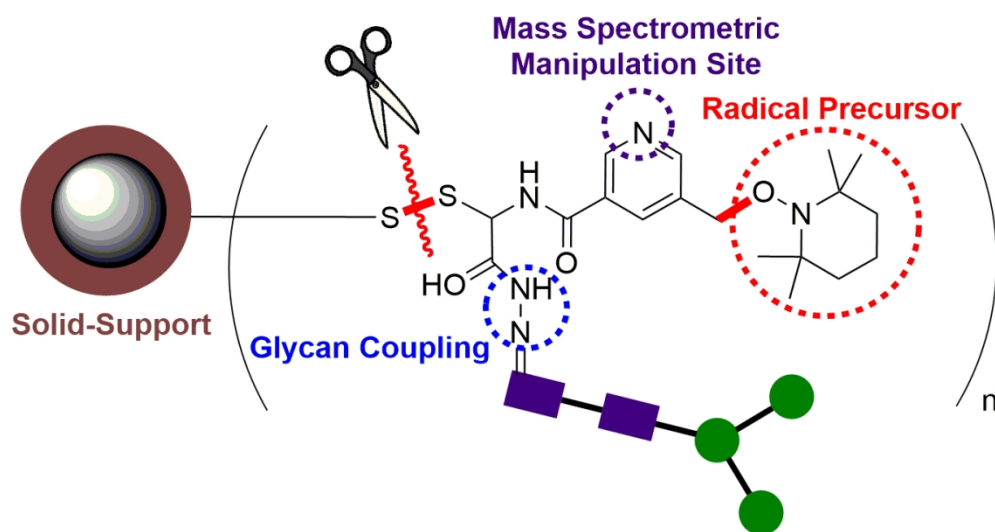
REFERENCE

1. Dennis, J. W.; Nabi, I. R.; Demetriou, M. Metabolism, cell surface organization, and disease. *Cell* **2009**, *139*, 1229-1241.
2. Liu, F. T.; Bevins, C. L. A sweet target for innate immunity. *Nat. Med.* **2010**, *16*, 263-264.
3. Kaji, H.; Saito, H.; Yamauchi, Y.; Shinkawa, T.; Taoka, M.; Hirabayashi, J.; Kasai, K.; Takahashi, N.; Isobe, T. Lectin affinity capture, isotope-coded tagging and mass spectrometry to identify N-linked glycoproteins. *Nat. Biotechnol.* **2003**, *21*, 667-672.
4. Ueda, K.; Takami, S.; Saichi, N.; Daigo, Y.; Ishikawa, N.; Kohno, N.; Katsumata, M.; Yamane, A.; Ota, M.; Sato, T. A.; Nakamura, Y.; Nakagawa, H. Development of serum glycoproteomic profiling technique; simultaneous identification of glycosylation sites and site-specific quantification of glycan structure changes. *Mol. Cell Proteomics* **2010**, *9*, 1819-1828.
5. Vandenborre, G.; Van Damme, E. J.; Ghesquiere, B.; Menschaert, G.; Hamshou, M.; Rao, R. N.; Gevaert, K.; Smagghe, G. Glycosylation signatures in Drosophila: fishing with lectins. *J. Proteome Res* **2010**, *9*, 3235-3242.
6. Zielinska, D. F.; Gnad, F.; Wisniewski, J. R.; Mann, M. Precision Mapping of an In Vivo N-Glycoproteome Reveals Rigid Topological and Sequence Constraints. *Cell* **2010**, *141*, 897-907.
7. Rudd, P. M.; Guile, G. R.; Kuster, B.; Harvey, D. J.; Opdenakker, G.; Dwek, R. A. Oligosaccharide sequencing technology. *Nature* **1997**, *388*, 205-207.
8. De Boer, A. R.; Hokke, C. H.; Deelder, A. M.; Wührer, M. Serum antibody screening by surface plasmon resonance using a natural glycan microarray. *Glycoconjugate J.* **2008**, *25*, 75-84.
9. Ruhaak, L. R.; Huhn, C.; Waterreus, W. J.; De Boer, A. R.; Neususs, C.; Hokke, C. H.; Deelder, A. M.; Wührer, M. Hydrophilic interaction chromatography-based high-throughput sample preparation method for N-glycan analysis from total human plasma glycoproteins. *Anal. Chem.* **2008**, *80*, 6119-6126.
10. Bereman, M. S.; Williams, T. I.; Muddiman, D. C. Development of a nanoLC LTQ orbitrap mass spectrometric method for profiling glycans derived from plasma from healthy, benign tumor control, and epithelial ovarian cancer patients. *Anal. Chem.* **2009**, *81*, 1130-1136.
11. Huang, H. X.; Jin, Y.; Xue, M. Y.; Yu, L.; Fu, Q.; Ke, Y. X.; Chu, C. H.; Liang, X. M. A novel click chitooligosaccharide for hydrophilic interaction liquid chromatography. *Chem. Commun.* **2009**, *45*, 6973-6975.
12. Bones, J.; Mittermayr, S.; O'Donoghue, N.; Guttman, A.; Rudd, P. M. Ultra performance liquid chromatographic profiling of serum N-glycans for fast and efficient identification of cancer associated alterations in glycosylation. *Anal. Chem.* **2010**, *82*, 10208-15.

13. Selman, M. H.; Hemayatkar, M.; Deelder, A. M.; Wuhler, M. Cotton HILIC SPE microtips for microscale purification and enrichment of glycans and glycopeptides. *Anal. Chem.* **2011**, *83*, 2492-2499.
14. Ruhaak, L. R.; Miyamoto, S.; Kelly, K.; Lebrilla, C. B. N-Glycan profiling of dried blood spots. *Anal. Chem.* **2012**, *84*, 396-402.
15. Packer, N. H.; Lawson, M. A.; Jardine, D. R.; Redmond, J. W. A general approach to desalting oligosaccharides released from glycoproteins. *Glycoconj J.* **1998**, *15*, 737-47.
16. Larsen, M. R.; Hojrup, P.; Roepstorff, P. Characterization of gel-separated glycoproteins using two-step proteolytic digestion combined with sequential microcolumns and mass spectrometry. *Mol. Cell Proteomics* **2005**, *4*, 107-119.
17. Zatsepin, T. S.; Stetsenko, D. A.; Arzumanov, A. A.; Romanova, E. A.; Gait, M. J.; Oretskaya, T. S. Synthesis of peptide-oligonucleotide conjugates with single and multiple peptides attached to 2'-aldehydes through thiazolidine, oxime, and hydrazine linkages. *Bioconjugate Chem.* **2002**, *13*, 822-830.
18. Guillaumie, F.; Justesen, S. F. L.; Mutenda, K. E.; Roepstorff, P.; Jensen, K. J.; Thomas, O. R. T. Fractionation, solid-phase immobilization and chemical degradation of long pectin oligogalacturonides. Initial steps towards sequencing of oligosaccharides. *Carbohydr. Res.* **2006**, *341*, 118-129.
19. Larsen, K.; Thygesen, M. B.; Guillaumie, F.; Willats, W. G.; Jensen, K. J. Solid-phase chemical tools for glycobiology. *Carbohydr. Res.* **2006**, *341*, 1209-1234.
20. Abe, M.; Shimaoka, H.; Fukushima, M.; Nishimura, S. I. A cross-linked polymer possessing a high density of hydrazide groups: high-throughput glycan purification and labeling for high-performance liquid chromatography analysis. *Polym. J.* **2012**, *44* (3), 269-277.
21. Yang, S. J.; Zhang, H. Glycan Analysis by Reversible Reaction to Hydrazide Beads and Mass Spectrometry. *Anal. Chem.* **2012**, *84*, 2232-2238.
22. Bai, H.; Pan, Y.; Tong, W.; Zhang, W.; Ren, X.; Tian, F.; Peng, B.; Wang, X.; Zhang, Y.; Deng, Y.; Qin, W.; Qian, X. Graphene based soft nanoreactors for facile "one-step" glycan enrichment and derivatization for MALDI-TOF-MS analysis. *Talanta* **2013**, *117*, 1-7.
23. Yang, S.; Yuan, W.; Yang, W. M.; Zhou, J. Y.; Harlan, R.; Edwards, J.; Li, S. W.; Zhang, H. Glycan Analysis by Isobaric Aldehyde Reactive Tags and Mass Spectrometry. *Anal. Chem.* **2013**, *85*, 8188-8195.
24. Sun, N.; Deng, C.; Li, Y.; Zhang, X. Highly selective enrichment of N-linked glycan by carbon-functionalized ordered graphene/mesoporous silica composites. *Anal. Chem.* **2014**, *86*, 2246-2250.
25. Jang, K. S.; Nani, R. R.; Kalli, A.; Levin, S.; Muller, A.; Hess, S.; Reisman, S. E.; Clemons, W. M. A cationic cysteine-hydrazide as an enrichment tool for the mass spectrometric characterization of bacterial free oligosaccharides. *Anal. Bioanal. Chem.* **2015**, *407*, 6181-6190.
26. Gao, J.; Thomas, D. A.; Sohn, C. H.; Beauchamp, J. L. Biomimetic reagents for the selective free radical and acid-base chemistry of glycans: application to glycan structure determination by mass spectrometry. *J. Am. Chem. Soc.* **2013**, *135*, 10684-10692.
27. Varki, A. C.; Esko, J. D.; Freeze, H. H.; Stanley, P.; Bertozzi, C. R.; Hart, G. W.; Etzler, M. E., *Essentials of Glycobiology*, 2nd edition. Cold Spring Harbor Laboratory Press: 2009.
28. Harvey, D. J. Ionization and collision-induced fragmentation of N-linked and related carbohydrates using divalent cations. *J. Am. Soc. Mass Spectrom.* **2001**, *12*, 926-937.
29. Adamson, J. T.; Hakansson, K. Electron capture dissociation of oligosaccharides ionized with alkali, alkaline earth, and transition metals. *Anal. Chem.* **2007**, *79*, 2901-2910.
30. Tykesson, E.; Mao, Y.; Maccarana, M.; Pu, Y.; Gao, J. S.; Lin, C.; Zaia, J.; Westergren-Thorsson, G.; Ellervik, U.; Malmstrom, L.; Malmstrom, A. Deciphering the mode of action of the processive polysaccharide modifying enzyme dermatan sulfate epimerase 1 by hydrogen-deuterium exchange mass spectrometry. *Chem. Sci.* **2016**, *7*, 1447-1456.

31. Xie, Y. M.; Lebrilla, C. B. Infrared multiphoton dissociation of alkali metal-coordinated oligosaccharides. *Anal. Chem.* **2003**, *75*, 1590-1598.
32. Harvey, D. J.; Bateman, R. H.; Green, M. R., High-energy Collision-induced Fragmentation of Complex Oligosaccharides Ionized by Matrix-assisted Laser Desorption/Ionization Mass Spectrometry. *J. Mass Spectrom.* **1997**, *32*, 167-187.
33. Zhang, L.; Reilly, J. P. Extracting Both Peptide Sequence and Glycan Structural Information by 157 nm Photodissociation of N-Linked Glycopeptides. *J. Proteome Res.* **2009**, *8*, 734-742.
34. Ko, B. J.; Brodbelt, J. S. 193 nm Ultraviolet Photodissociation of Deprotonated Sialylated Oligosaccharides. *Anal. Chem.* **2011**, *83*, 8192-8200.
35. Brodbelt, J. S. Photodissociation mass spectrometry: new tools for characterization of biological molecules. *Chem. Soc. Rev.* **2014**, *43*, 2757-2783.
36. Budnik, B. A.; Haselmann, K. F.; Elkin, Y. N.; Gorbach, V. I.; Zubarev, R. A. Applications of electron-ion dissociation reactions for analysis of polycationic chitooligosaccharides in Fourier transform mass spectrometry. *Anal. Chem.* **2003**, *75*, 5994-6001.
37. Zhao, C.; Xie, B.; Chan, S. Y.; Costello, C. E.; O'Connor, P. B. Collisionally activated dissociation and electron capture dissociation provide complementary structural information for branched permethylated oligosaccharides. *J. Am. Soc. Mass Spectrom.* **2008**, *19*, 138-150.
38. Huang, Y. Q.; Pu, Y.; Yu, X.; Costello, C. E.; Lin, C. Mechanistic Study on Electron Capture Dissociation of the Oligosaccharide-Mg²⁺ Complex. *J. Am. Soc. Mass Spectrom.* **2014**, *25*, 1451-1460.
39. Wolff, J. J.; Leach, F. E.; Laremore, T. N.; Kaplan, D. A.; Easterling, M. L.; Linhardt, R. J.; Amster, I. J. Negative Electron Transfer Dissociation of Glycosaminoglycans. *Anal. Chem.* **2010**, *82*, 3460-3466.
40. Han, L.; Costello, C. Electron Transfer Dissociation of Milk Oligosaccharides. *J. Am. Soc. Mass Spectrom.* **2011**, *22*, 997-1013.
41. Kornacki, J. R.; Adamson, J. T.; Hakansson, K. Electron Detachment Dissociation of Underivatized Chloride-Adducted Oligosaccharides. *J. Am. Soc. Mass Spectrom.* **2012**, *23*, 2031-2042.
42. Kailemia, M. J.; Park, M.; Kaplan, D. A.; Venot, A.; Boons, G. J.; Li, L. Y.; Linhardt, R. J.; Amster, I. J. High-Field Asymmetric-Waveform Ion Mobility Spectrometry and Electron Detachment Dissociation of Isobaric Mixtures of Glycosaminoglycans. *J. Am. Soc. Mass Spectrom.* **2014**, *25*, 258-268.
43. Tang, Y.; Pu, Y.; Gao, J. S.; Hong, P. Y.; Costello, C. E.; Lin, C. De Novo Glycan Sequencing by Electronic Excitation Dissociation and Fixed-Charge Derivatization. *Anal. Chem.* **2018**, *90*, 3793-3801.
44. Yu, X.; Jiang, Y.; Chen, Y. J.; Huang, Y. Q.; Costello, C. E.; Lin, C. Detailed Glycan Structural Characterization by Electronic Excitation Dissociation. *Anal. Chem.* **2013**, *85*, 10017-10021.
45. Huang, Y. Q.; Pu, Y.; Yu, X.; Costello, C. E.; Lin, C. Mechanistic Study on Electronic Excitation Dissociation of the Cellobiose-Na⁺ Complex. *J. Am. Soc. Mass Spectrom.* **2016**, *27*, 319-328.
46. Gao, J. S.; Jankiewicz, B. J.; Reece, J.; Sheng, H. M.; Cramer, C. J.; Nash, J. J.; Kenttamaa, H. I. On the factors that control the reactivity of meta-benzynes. *Chem. Sci.* **2014**, *5*, 2205-2215.
47. Riggs, D. L.; Hofmann, J.; Hahm, H. S.; Seeberger, P. H.; Pagel, K.; Julian, R. R. Glycan Isomer Identification Using Ultraviolet Photodissociation Initiated Radical Chemistry. *Anal. Chem.* **2018**, *90*, 11581-11588.
48. Sohn, C. H.; Gao, J. S.; Thomas, D. A.; Kim, T. Y.; Goddard, W. A.; Beauchamp, J. L. Mechanisms and energetics of free radical initiated disulfide bond cleavage in model peptides and insulin by mass spectrometry. *Chem. Sci.* **2015**, *6*, 4550-4560.
49. Turecek, F.; Julian, R. R. Peptide Radicals and Cation Radicals in the Gas Phase. *Chem. Rev.* **2013**, *113*, 6691-6733.
50. Zhang, X.; Julian, R. R. Radical mediated dissection of oligosaccharides. *Int. J. Mass Spectrom.* **2014**, *372*, 22-28.

51. Gaspar, K.; Fabijanczuk, K.; Otegui, T.; Acosta, J.; Gao, J. S. Development of Novel Free Radical Initiated Peptide Sequencing Reagent: Application to Identification and Characterization of Peptides by Mass Spectrometry. *J. Am. Soc. Mass Spectrom.* **2019**, *30*, 548-556.
52. Desai, N.; Thomas, D. A.; Lee, J.; Gao, J. S.; Beauchamp, J. L. Eradicating mass spectrometric glycan rearrangement by utilizing free radicals. *Chem. Sci.* **2016**, *7*, 5390-5397.
53. Katz, E.; Willner, I. Integrated nanoparticle-biomolecule hybrid systems: Synthesis, properties, and applications. *Angew. Chem. Int. Ed.* **2004**, *43*, 6042-6108.
54. Ma, M.; Wu, Y.; Zhou, H.; Sun, Y. K.; Zhang, Y.; Gu, N. Size dependence of specific power absorption of Fe₃O₄ particles in AC magnetic field. *J. Magn. Magnetic Mater.* **2004**, *268*, 33-39.
55. Safarik, I.; Safarikova, M. Magnetic techniques for the isolation and purification of proteins and peptides. *Biomagn. Res. Technol.* **2004**, *2*, 7.
56. Palani, A.; Lee, J. S.; Huh, J.; Kim, M.; Lee, Y. J.; Chang, J. H.; Lee, K.; Lee, S. W. Selective enrichment of cysteine-containing peptides using SPDP-Functionalized superparamagnetic Fe₃O₄@SiO₂ nanoparticles: Application to comprehensive proteomic profiling. *J. Proteome Res.* **2008**, *7*, 3591-3596.
57. Kim, J. S.; Dai, Z. Y.; Aryal, U. K.; Moore, R. J.; Camp, D. G.; Baker, S. E.; Smith, R. D.; Qian, W. J. Resin-Assisted Enrichment of N-Terminal Peptides for Characterizing Proteolytic Processing. *Anal. Chem.* **2013**, *85*, 6826-6832.
58. Lima-Tenorio, M. K.; Pineda, E. A. G.; Ahmad, N. M.; Fessi, H.; Elaissari, A. Magnetic nanoparticles: In vivo cancer diagnosis and therapy. *Int. J. Pharmaceut.* **2015**, *493*, 313-327.
59. Patil, U. S.; Qu, H. O.; Caruntu, D.; O'Connor, C. J.; Sharma, A.; Cai, Y.; Tarr, M. A. Labeling Primary Amine Groups in Peptides and Proteins with N-Hydroxysuccinimidyl Ester Modified Fe₃O₄@SiO₂ Nanoparticles Containing Cleavable Disulfide-Bond Linkers. *Bioconjugate Chem.* **2013**, *24*, 1562-1569.
60. Domon, B. C., C. E. A systematic nomenclature for carbohydrate fragmentations in FAB-MS/MS spectra of glycoconjugates. *Glycoconjugate J.* **1988**, *5*, 397-409.
61. Costello, C. E.; Contado-Miller, J. M.; Cipollo, J. F. A Glycomics Platform for the Analysis of Permethylated Oligosaccharide Alditols. *J. Am. Soc. Mass Spectrom.* **2007**, *18*, 1799-1812.
62. Prien, J. M.; Ashline, D. J.; Lapadula, A. J.; Zhang, H.; Reinhold V. N. The High Mannose Glycans from Bovine Ribonuclease B Isomer Characterization by Ion Trap MS. *J. Am. Soc. Mass Spectrom.* **2009**, *20*, 539-556.



116x62mm (300 x 300 DPI)